

Rand Protease: The Role of Calcium-Binding Site on Stability with Mutagenesis and the Effectiveness on Leather Dehairing

(Rand Protease: Peranan Tapak Pengikat Kalsium terhadap Kestabilan dengan Mutagenesis dan Keberkesanan terhadap Penyahbuluan Kulit)

PHANG ZI WEI¹, NUR ALIYAH MOHD AZRIN², MOHD SHUKURI MOHAMAD ALI^{1,2} & NOOR DINA MUHD NOOR^{1,2,*}

¹*Department of Biochemistry, Faculty of Biotechnology and Biomolecular Sciences, Universiti Putra Malaysia, 43400 UPM Serdang, Selangor, Malaysia*

²*Enzyme and Microbial Research Center, Faculty of Biotechnology & Biomolecular Sciences, Universiti Putra Malaysia, 43400 UPM Serdang, Selangor, Malaysia*

Received: 7 May 2023/Accepted: 21 December 2023

ABSTRACT

Bacillus subtilis produces a number of proteases, which are highly demanded in various industries, especially the thermostable one. Rand protease, originally isolated from *B. subtilis*, has thermostability and other remarkable properties such as organic solvent tolerance and pH stability. However, its vulnerability to instability-induced degradation has limited its applications. Because Rand protease contains two calcium ions for folding, activation, and, above all, stability, previous studies have shown that boosting the calcium-binding affinity enhances stability. Therefore, Rand protease's susceptibility to degradation could be remedied by discovering the calcium-binding site having the greatest impact on stability for further calcium-binding affinity improvement. This was done with an *in silico* mutagenesis approach whereby one calcium-binding site was mutated to alanine and evaluated either the RMSD, the deviation of the mutated configuration from the original configuration using YASARA, or stability in terms of kcal/mol using HotSpot Wizard. The result found that calcium-binding sites Leu75 from YASARA and Tyr171 from HotSpot Wizard have higher influences on stability (our target). This result was also validated using Pymol, ExpASY ProtParam, and Molprobit. Additionally, Rand protease-chemical formulation dehaired leather best without additional metal ions at pH 7.0 and for 18 h. It also produced higher-quality leather with smaller pores and softer leather than chemical formulations. In contrast, hair breakage was observed in calcium treatment, which is compatible with the low dehairing activity achieved. In conclusion, Leu75 and Tyr171 are vital for calcium stabilisation and this enzyme has demonstrated its crucial efficacy in the leather dehairing industry.

Keywords: Calcium-binding site; Leather dehairing industry; Rand protease; stability

ABSTRAK

Bacillus subtilis menghasilkan sejumlah protease yang amat diperlukan dalam pelbagai industri, terutamanya yang berkaitan dengan kestabilan terma. Protein Rand yang dipencilkan daripada *B. subtilis* mempunyai kestabilan terma dan ciri luar biasa lain seperti toleransi terhadap pelarut organik dan kestabilan pH. Walau bagaimanapun, kelemahannya terhadap degradasi akibat ketidakstabilan telah mengehadkan penggunaannya. Oleh kerana protein Rand mengandungi dua ion kalsium untuk lipatan, pengaktifan dan yang paling penting sekali kestabilan, kajian terdahulu telah menunjukkan bahawa peningkatan keafinan pengikat kalsium mampu meningkatkan kestabilan. Oleh itu, kerentanan protein Rand terhadap degradasi boleh diperbaiki dengan meneliti tapak pengikat kalsium yang mempunyai kesan paling besar terhadap kestabilan untuk menambahbaik keafinan pengikat kalsium. Ini boleh dilakukan dengan pendekatan mutagenesis secara *in silico* dengan satu tapak pengikat kalsium dimutasi kepada alanina dan penilaiannya dilakukan sama ada daripada segi RMSD, sisihan konfigurasi bermutasi daripada konfigurasi asal menggunakan YASARA, atau daripada segi kestabilan, kcal/mol menggunakan HotSpot Wizard. Hasilnya, didapati bahawa tapak pengikat kalsium Leu75 daripada YASARA dan Tyr171 daripada HotSpot Wizard, mempunyai pengaruh yang lebih tinggi terhadap kestabilan (sasaran) berbanding tapak pengikat kalsium yang lain. Keputusan ini juga

telah disahkan menggunakan Pymol, ExPASy ProtParam dan Molprobit. Tambahan pula, formulasi kimia protein Rand mengenyah kulit dengan baik tanpa ion logam tambahan pada pH 7.0, selama 18 jam. Ia juga menghasilkan kulit berkualiti tinggi seperti liang pori yang lebih kecil dan kulit yang lebih lembut berbanding formulasi kimia. Selain itu, tahap kepatahan rambut yang turut diperhatikan dalam rawatan kalsium, menunjukkan keserasian apabila aktiviti penyahbuluan kulit mencapai tahap yang rendah. Kesimpulannya, Leu75 dan Tyr171 adalah penting untuk penstabilan kalsium dan enzim ini telah menunjukkan keberkesannya yang penting dalam industri penyahbuluan kulit.

Kata kunci: Industri penyahbuluan kulit; kestabilan; protein Rand; tapak pengikat kalsium

INTRODUCTION

Nowadays, enzymes are mostly used in place of chemicals in industry as environmental concerns continue to escalate. This condition increased the commercial value of several enzymes, such as protease, cellulase, lactase, and catalase. Protease accounts for a significant share of the entire industrial enzyme (60%), with annual sales of around 1.8 billion US dollars (Ward, 2011). Netherlands, Germany, and India were among the top importers (Volza Grow Global, 2023). Furthermore, the reading is projected to rise in the next five years, particularly for microbial protease (Suraj & Onkar 2022). Microbial proteases are favoured due to their rapid production capabilities within a restricted timeframe, along with their efficiency, controllability, and cost-effectiveness. Protease encompasses several families, including aspartic acid protease, asparagine protease, cysteine protease, metalloprotease, glutamic acid protease, threonine protease, and serine protease. Within this diverse range, a well-established group of microbial serine proteases, subtilisin, distinguishes itself for its exceptional thermostability, compatibility with high pH conditions, and valuable role as an additive in detergents. This versatility has led to subtilisin's utilisation across various industries like textiles, leather, food processing, pharmaceutical synthesis, and wastewater treatment (Azrin et al. 2022).

One of the major limitations inherent in all enzymes, including Rand protease (a subtilisin), is that although they are able to tolerate a certain range of temperature, pH, and other conditions for their best performance, they degrade when encountering unfavourable environments. Enzymes can sometimes denature irreversibly, resulting in massive industrial losses and limiting their use in industry. As a result, enzymes are frequently regarded as unstable. It is due to this challenge that stability has garnered great attention from researchers throughout the years, with mutagenesis emerging as one of the promising

solutions (Califano & Costantini 2021; Gianfreda & Scarfi 1991).

Bacillus subtilis strain Rand had previously been isolated and was considered to be the first production of a thermostable and organic solvent-tolerant protease (Abusham et al. 2009). This subtilisin (Rand protease) is composed of three catalytic triads (Asp32, His64, and Ser221), two calcium binding sites (high- and low-affinity), and 275 mature amino acid residues. The high-affinity (Ca1) and low-affinity (Ca2) calcium metals were closely linked to stability, ensuring proper activation. During activation, the partially folded peptide chain was equipped with a Ca2 binding site only inside the cytosol. This is due to the subtilisin's unstable conformation in the absence of Ca2 and the Gln2 binding residue being distant from the Ca1 site. Hence, the Ca1 binding site is only formed after Ca2 attachment to stabilise the structure and enable propeptide detachment, resulting in conformational changes. Ca1 binds more specifically and strongly than Ca2, fully stabilising the structure and completing the folding and activation. The calcium-binding residues for Ca1 and Ca2 were previously discovered to be Tyr171, Ala169, Thr174, Asp197 (for Ca1), and Gln2, Asp41, Leu75, Ile79, Asn77, Val81 (for Ca2). The effects of each calcium-binding residue on stability, however, remain unknown. Therefore, our goal is to employ *in silico* mutagenesis using YASARA and HotSpot Wizard to identify the most important calcium-binding sites for improving stability.

In addition, this study investigates the potential of Rand protease in the leather industry. Conventional leather dehairing contributes significantly to chemical contamination, with 65-70% of contaminants originating from lime sulfite. The global sulfur pollution in 2019 was estimated to be around 22,076 kilotonnes, and the lime market in 2021 was valued at approximately 40.07 billion US dollars (Vlavianos 2020). Hence, it is important for greener leather dehairing process to be employed in

order to reduce pollution and manufacture smoother skin products, as evidenced by Suharti et al. (2018). In this study, Rand protease was characterised and optimised to evaluate its dehairing capabilities. Since other subtilisins have previously demonstrated their dehairing activity, Rand protease (a subtilisin) may exhibit superior performance in terms of skin quality and activity rate.

In our study, we aimed to identify the most critical calcium-binding site through *in silico* approaches, which may enhance the stability of Rand protease and broaden its commercial applicability in the future. Our second objective was to determine the optimal conditions for Rand protease to collaborate with lime sulfite in leather dehairing, as opposed to other conventional formulations.

MATERIALS AND METHODS

in silico STUDY FOR CALCIUM-BINDING SITE DETERMINATION

Homology Modelling (SWISS-MODEL)

A mature amino acid sequence of Rand protease was obtained from NCBI and inputted into the SWISS-MODEL server. A template was chosen, and the 3D structure was predicted. Afterwards, structure validation was done using UCLA-DOE LAB (<https://saves.mbi.ucla.edu/>), ProSA-web (<https://prosa.services.came.sbg.ac.at/prosa.php>), and MolProbity (<http://molprobity.biochem.duke.edu/index.php>). Later, the calcium-binding sites were determined through alignment of the Rand protease sequence retrieved from NCBI with a sequence of highest similarity and known calcium-binding sites in Uniprot.

Molecular Docking (YASARA)

Global docking was done on the original 3D structure (wild type) and the substrate (N-succinyl-alanyl-alanyl-prolyl-phenylalanine-4-nitroanilide) using YASARA software, followed by the nine possible calcium-binding site mutations with the substrate. All nine possible calcium-binding sites were substituted by alanine (A). The substrate was chosen based on Abusham et al. (2019). For each dock, one result was selected. The single docking result chosen for each mutation was then superimposed on the single docking result chosen for the wild type. The RMSD values for each mutation were obtained.

HotSpot Wizard

On the HotSpot Wizard website (<https://loschmidt.chemi.muni.cz/hotspotwizard/>), the 3D model was submitted.

In accordance with the preferred mutation type (single-point mutation to alanine), the selected amino acid residues underwent stability screening. Lastly, the results from both YASARA and HotSpot Wizard were analysed with Pymol (<http://www.pymol.org/pymol>) and ExPASy ProtParam for 3D structure analysis and data support (Schrödinger & DeLano 2020).

CHARACTERISATION OF RAND PROTEASE FOR LEATHER DEHAIRING

Crude Enzyme Production

The bacteria culture was spread on pH 7, 2% skim milk agar (SMA) plates and incubated at 37 °C overnight. A single colony transferred into 10 mL of sterile nutrient broth (pH 7) and grown at 37 °C for 12 h at agitation speed of 150 rpm was used as seed culture. Then, 4 mL of the seed culture was inoculated into 200 mL of production media (CaCl₂·2H₂O (0.5 g/L), K₂HPO₄ (0.2 g/L), MgSO₄·7H₂O (0.5 g/L), NaCl (0.1 g/L), and tryptone (1% w/v)) and incubated under the same conditions as mentioned. The cell-free supernatant was recovered after centrifugation at 8000 rpm for 20 mins at 4 °C (Abusham et al. 2009; Hakim et al. 2018).

Heat Treatment and Spin Concentration

The cell-free supernatant was heat-treated for 20 min at 50 °C and immediately chilled on ice for 10 min. Then, it was centrifuged at 12000 × g for 10 min. To increase the concentration of enzymes, 5 mL supernatant was pipetted into the 15 mL sample reservoir of Pall spin concentrator to be centrifuged at 14000 × g, 30 mins at 4 °C. The enzyme retained was recovered (Jung et al. 2023; Mehrnoush, Mustafa & Yazid 2011).

Bradford Assay

Prior to the experiment, protein was measured using the method suggested by Bradford (1976), with bovine serum albumin as the standard.

Protease Activity Assay

The protease activity was determined by a slight modification method proposed by Shaikh, Dixit and Shaikh (2018). A test tube with 1 mL of pre-prepared substrate azocasein solution (0.5% w/v) in 0.1 M Tris-HCl buffer (pH 7.0) was pre-warmed to 50 °C. The reaction was initiated by adding 100 µL of the enzyme solution into the azocasein solution and incubating at 50 °C for 30 min at 150 rpm. An equal volume of 10% (w/v)

trichloroacetic acid was added. The mixture was left to stand at room temperature for 30 min and centrifuged for 10 min at $13000 \times g$. One mL of supernatant was then transferred and mixed with an equal volume of NaOH (1 M). The absorbance was read at 450 nm. Each sample was run in triplicate. As a control, the enzyme was added at the end of the incubation period. One unit of protease activity is defined in the assay conditions, which give an increase of 0.001 absorbance units at 450 nm per min.

SDS-PAGE

The molecular weight and purity of the protein were analysed by a 10% SDS-PAGE, followed by staining with Coomassie Brilliant Blue (CBB). The 10% resolving gel solution was prepared, loaded into the gel casting tray, and solidified. Similarly, the 4% stacking gel solution was prepared and loaded onto the above-solidified casting tray. Prior to loading protein samples onto a well, the protein sample was mixed with the working buffer solution containing β -mercaptoethanol and boiled for 10 min. The gel was run at 130 V for 90 min, followed by CBB staining, destaining, and finally band observation (Abusham et al. 2009).

Dehairing Optimisation

The cow skin was cleaned with water and cut into square pieces of $5 \times 5 \text{ cm}^2$. One piece of cow skin was dipped in partially purified enzymes, 7% (w/v) sodium sulfite, and 7% (w/v) lime for 5 min before incubation. For the negative controls, cow skin was treated with distilled water. To investigate the significance of chemicals in the process, the cow skins were treated with 7% (w/v) sodium sulfite and 7% (w/v) lime, 7% (w/v) sodium sulfite only, and 7% (w/v) lime only. All treatments had their pH and temperatures set to 7.0 and 50 °C, respectively, for 12 h. After the treatment, the depilation process was assessed by weighing the amount of hair removed in grams and observing the general appearance of the leather surface using a skin analyser. The condition of the hair was viewed under a light microscope (Hakim et al. 2018; Mukhtar & Haq 2008).

For determination of the optimal incubation times, the cow skin was incubated for 18 h and 24 h, after a 5-min immersion in partially purified enzymes, 7% (w/v) sodium sulfite, and 7% (w/v) lime. All pH and temperatures were set to 7.0 and 50 °C, respectively. Following the treatment, the depilation process was assessed as before (Hakim et al. 2018; Mukhtar & Haq 2008).

For metal ions (Ca^{2+} , Zn^{2+}) determination, a 10 mM metal ion in a 50 mM Tris-HCl buffer was added to a solution of partially purified enzyme, 7% (w/v) sodium sulfite, and 7% (w/v) lime. The tested metal salts were CaCl_2 and ZnCl_2 . The cow skin was treated for 5 min before incubation. All pH, temperatures, and incubation times were set to 7.0, 50 °C, and 12 h, respectively. Similarly, the depilation process was assessed as above (Hakim et al. 2018; Mukhtar & Haq 2008).

For pH optimization, the treatments were adjusted to pH 9.0 and 11.0. The cow skin was dipped in partially purified enzymes, 7% (w/v) sodium sulfite, and 7% (w/v) lime for 5 min before incubation. All treatments were conducted at a temperature of 50°C for 12 h. Similarly, the depilation process was assessed as above (Hakim et al. 2018; Mukhtar & Haq 2008).

RESULTS AND DISCUSSION

In silico STUDY FOR CALCIUM-BINDING SITE DETERMINATION

The Rand protease sequence was retrieved from NCBI, where it is in the form of pre-pro peptide and mature sequence combinations. The mature sequence was used for SWISS-MODEL structure prediction. The result showed that Rand protease consists of 6 α -helices and 13 β -strands (Figure 1). Afterwards, our model was validated with UCLA-DOE LAB (ERRAT, VERIFY3D, and PROCHECK), ProSA-Web, and MolProbity. Our model was proven to be high-quality, and the number of residues in the most favoured region is acceptable (Table 1).

The calcium-binding sites were discovered by aligning a sequence (B0FXJ2) with known calcium-binding sites and high percentage identity (71.7%) to Rand protease in Uniprot. The results obtained for calcium-binding sites of Rand protease were Gln2, Asp41, Leu75, Asn77, Ile79, Val81, Ala169, Tyr171, and Thr174, which were also discovered by Abusham et al. (2019). An additional calcium-binding site on Asp197 was also observed. All the possible calcium-binding sites were brought forward for molecular docking and HotSpot Wizard analysis.

In molecular docking, one out of twenty-five outcomes was selected based on criteria: the catalytic triad (Asp32, His64, and Ser221), higher binding energy, and contacting receptor residues. The greater binding energy in docking was associated with stronger ligand-receptor binding (Mohanty & Mohanty 2023). According to Table 2, manually changing Leu75 produced the largest

RMSD, possibly as a result of the change's distance to Asp41. Leu75 and Ile79 connect other calcium-binding sites to Asp41, thus forming a circle-like bond structure with calcium. Asp41 has a closer distance of 3.5 Å to Leu75 as compared to 3.9 Å to Ile79, which gives it a more significant role in terms of stability (Figure 2.1A). Mutation to Ala weakens the bond from 3.5 Å (Leu75) to 3.7 Å (Ala) between Asp41 and Leu/Ala (Figure 2.1B). This data was further corroborated by HotSpot mutation, resulting in a 2.6 kcal/mol reduction in stability (Table 2). Thus, the most influential calcium-binding site on stability (our target) may be amino acid 75 (Schrödinger & DeLano 2020; Sumbalova et al. 2018).

On the contrary, the highest destabilisation, 5.7 kcal/mol, is generated at Tyr171 by HotSpot Wizard. This is because the Tyr171 side chain has a close interaction with Leu135, which is conserved in both hyperthermophilic and mesophilic subtilisin

(Figure 2.2A). This interaction strongly affects calcium stabilisation. This statement is proven when mutations on both Tyr171 and Leu135 to a further distance turn out to cause destabilisation in HotSpot Wizard (Table 2). Similarly, mutation to Ala further the distance between the interactions, thus disrupting stabilisation (Figure 2.2B). Moreover, Tyr171 is very distantly related to Ala. They have a Grantham's distance of 112, causing vast changes in polarity, composition, and molecular volume after mutation (Grantham 1974). In addition, the YASARA mutation and ExPASy ProtParam also supported this data with a high RMSD value of 1.1965 Å and an increased instability index of 0.18, respectively (Table 2) (Schrödinger & DeLano 2020; Sumbalova et al. 2018).

In terms of better stabilisation, the Val81 mutation has the lowest RMSD of 0.2548 Å. These insignificant alterations might be attributed to the structural similarities of Val and Ala, as both are non-polar amino acids with

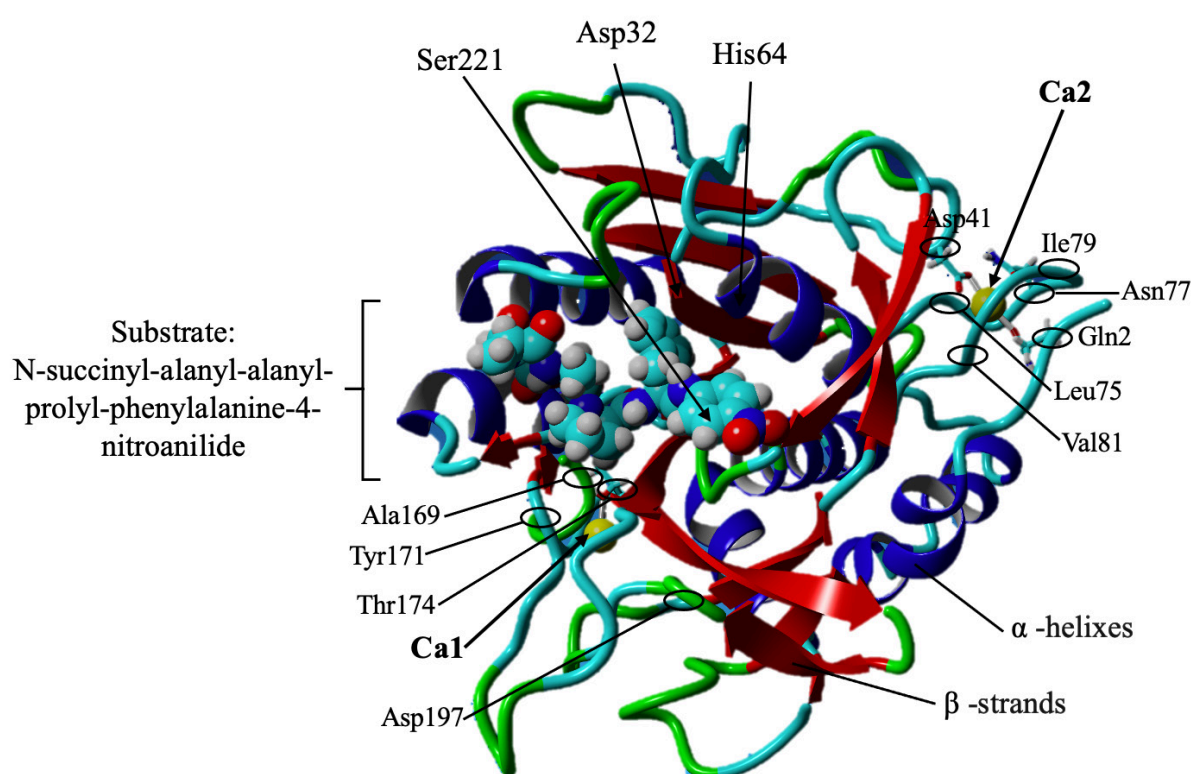


FIGURE 1. Predicted 3D structure of *B. subtilis* Rand protease in YASARA. The Rand protease is docked with its substrate on the catalytic triad of Asp32, His64, and Ser221. There are eight dark blue α -helices and fourteen red β -strands visible. The two calcium metals are depicted in yellow. The calcium-binding residues for Ca1 were Ala169, Tyr171, Thr174, and Asp197, while for Ca2 they were Gln2, Asp41, Leu75, Asn77, Ile79, and Val81

a very low Grantham's distance of 64 (Grantham 1974; Pal & Mitra 2022). However, the results from Pymol and HotSpot Wizard demonstrated no change in distance and a 3.4 kcal/mol destabilisation, respectively, which was incompatible with the result (Figure 2.3). Therefore, mutation of Val81 was concluded to be less vital for stability and caused no stability improvement (Gasteiger et al. 2005; Schrödinger & DeLano 2020; Sumbalova et al. 2018).

For the HotSpot Wizard, Asp41 was shown to be the only improved stability with -0.8 kcal/mol. This may be due to the clashing (steric collision) mentioned in the Molprobit structure evaluation and demonstrated in Pymol. The six possible conformations of His39 clash in all conformations with Asp41, while mutating to Ala showed one conformation with no clashing (Figure 2.4).

These data were supported by a low 0.4599 Å RMSD from the YASARA mutation (Chen et al. 2010; Gasteiger et al. 2005; Schrödinger & DeLano 2020; Sumbalova et al. 2018).

In summary, the YASARA and HotSpot Wizard webserver have demonstrated efficacy in localising important calcium-binding sites. Both methods identified Leu75 and Ty171 as critical calcium-binding sites. However, the YASARA method was found to be less effective in stabilisation determination. This limitation can be attributed to the possibility that even minor RMSD values (i.e., deviations from the original template) could indicate destabilisation mutations and vice versa. Therefore, when considering speed and efficacy, HotSpot Wizard would be a better option for stabilisation evaluation (Bendl et al. 2016).

TABLE 1. Summary from validation tools

Validation Tools	Results	Valid / Invalid
1. UCLA-DOE LAB		
a) ERRAT	<ul style="list-style-type: none"> High quality factor of 96.6038 	Valid
b) VERIFY3D	<ul style="list-style-type: none"> 80% compatibility of 3D structure to 1D structure Ramachandran plot <ul style="list-style-type: none"> 100% residues in allowed region 	Valid
c) PROCHECK	<ul style="list-style-type: none"> 88.5% residues in most favoured region G factor (-0.21) 	Valid
2. ProSA-web	<ul style="list-style-type: none"> z-score of -9.52 0% poor rotamers 1 Ramachandran outlier 96.7% favoured Ramachandran conformation 2 bad bonds 16 bad angels 	Valid
3. MolProbit	<ul style="list-style-type: none"> 4 clashing sites <ul style="list-style-type: none"> Val150 & Thr224 Val150 & Val227 His39 & Asp41 Val26 & Ala232 	Valid

TABLE 2. Summary output of manually mutation (YASARA) and single-point mutations from the HotSpot program

Position	Residue	Mutation	Manually (YASARA)		HotSpot Wizard	
			Ligand	RMSD Value (Å)	Stability (kcal/ mol)	Increase/ Decrease
Calcium-binding sites						
2	Gln	Ala	Suc-aapf-pna	1.2094	1.6	Decrease
41	Asp	Ala	Suc-aapf-pna	0.4599	-0.8	Increase
75	Leu	Ala	Suc-aapf-pna	1.3634	2.6	Decrease
77	Asn	Ala	Suc-aapf-pna	0.3897	1.0	Decrease
79	Ile	Ala	Suc-aapf-pna	0.3742	0.1	Decrease
81	Val	Ala	Suc-aapf-pna	0.2548	3.4	Decrease
171	Tyr	Ala	Suc-aapf-pna	1.1965	5.7	Decrease
174	Thr	Ala	Suc-aapf-pna	1.0607	1.0	Decrease
197	Asp	Ala	Suc-aapf-pna	0.3735	1.0	Decrease
Additional residue						
135	Leu	Ala	-	-	4.5	Decrease

APPLICATION OF RAND PROTEASE IN LEATHER DEHAIRING

In the second phase of the study, the capability of Rand protease to dehair leather was evaluated. The effectiveness of the heat treatment method on Rand protease purification was demonstrated, yielding a 1.9-fold increase and 16.9% yield. This purification method was employed due to its efficacy in eliminating heat-labile proteins (Ahmad, Tahir & Anjum 2020). The presence of Rand protease was further confirmed by the observation of a 28 kDa band on SDS-PAGE (data not shown) (Abusham et al. 2019).

Dehairing is essential in the leather industry to ensure that the hairs and epidermis are removed without damaging the leather. In our experiment, the 7% (w/v)

sodium sulfite with 7% (w/v) lime, 7% (w/v) sodium sulfite only, and 7% (w/v) lime only formulations were tested to identify the influence of chemicals on dehairing as compared to the enzyme-chemical mixture formulations: 0.00893 M partially purified Rand protease, 7% (w/v) sodium sulfite, and 7% (w/v) lime formulations. Table 3 presents the weight of cow skin after incubation and the weight of dehaired hair. The percentage of dehairing was calculated by dividing the weight of dehaired hair by the total weight of the skin (Zekeya et al. 2019). It was noted that enzyme-chemical treatment has the highest activity as compared to other chemical and control treatments. This finding demonstrates the significance of enzymes in dehairing activity, which has been supported by Mukhtar and Haq

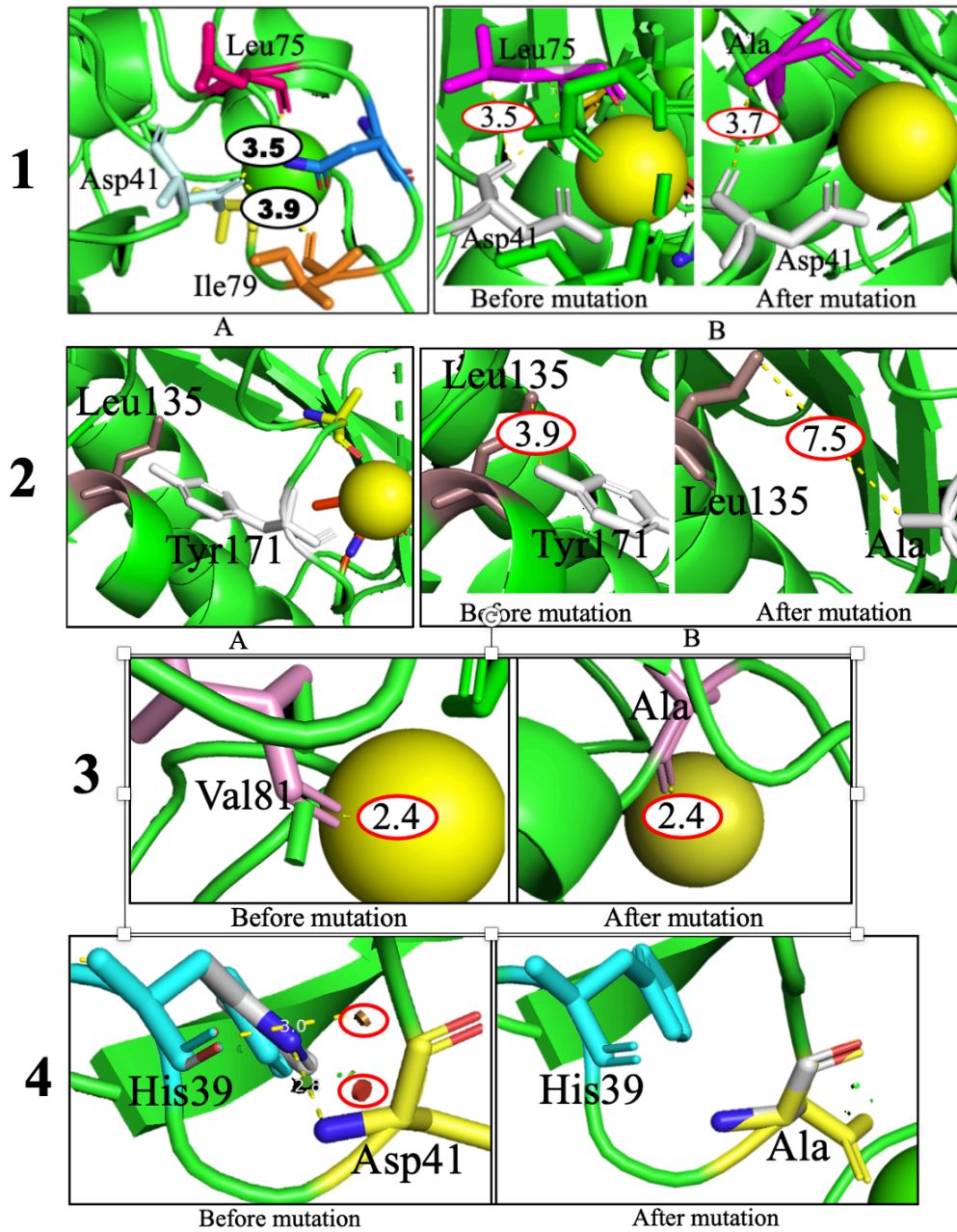


FIGURE 2. The supporting result from Pymol. (1A) The distances between Asp41 to Leu75, and Ile79 were circled in black. Leu75, Asp41, and Ile79 were highlighted in pink, light blue, and orange, respectively. (1B) The changes in distance before and after the mutation of Leu75 to alanine. The distances were circled in red. (2A) The position of Tyr171, Leu135, and calcium metal in Pymol. (2B) The changes in distance before and after the mutation of Tyr171 to alanine. The distances were circled in red. (3) The changes in distance before and after the mutation of Val81 to alanine. The distances were circled in red. (4) The changes before and after the mutation of Asp41 to alanine. The clashing sites were circled in red

(2008), who showed that enzyme-chemical treatment yields higher dehairing activity than either crude enzyme-only treatment or chemical-only treatment. Additionally, Figure 3(A) illustrates that enzyme-chemical treatment leads to higher-quality leather with smaller pores than sodium sulfite treatment. This desirable outcome is crucial for the leather dehairing industry (Eser & Aydemir 2022).

For sodium sulfite with lime treatment, the skin structure is damaged to a sticky configuration, making it impossible to define its dehairing activity (Figure 3(C)). This condition is indescribable, as goat skin in 14% lime sulfite after 6 h of incubation still show a firm structure, according to Mukhtar and Haq (2008), and goat skin dehairst faster than cattle skin due to its thinner proteinous layer (Zekeya et al. 2019). Furthermore, conventional dehairing takes 3-5 days at alkaline pH (above 12) (Sirvaityte, Vaitaisi & Jaimaines 2015; Thanikaivelan, Rao & Nair 2000). Hence, the skin was not supposed to be damaged within 12 h.

Regarding the effect of incubation times, the highest dehairing activity was observed at 18 h. To confirm this finding, a 24-h incubation period would be recommended for future studies. In terms of pH, the peak activity was observed at pH 7, which is consistent with the optimal pH for Rand protease activity (Abusham et al. 2019). With respect to metal influences, the addition of zinc outperformed calcium, but both were inferior to the absence of metal ions, as shown in Table 3. This result is expected, as calcium stabilises Rand protease and zinc activates it. However, certain serine proteases can be suppressed by zinc, which may account for the reduced dehairing activity of Rand protease in the presence of this metal (Ullah et al. 2022). Moreover, as lime sulfite (basic) reacts with acid, the acidic nature of CaCl_2 and ZnCl_2 interferes with the lime sulfite action in dehairing (Chapman 2018).

TABLE 3. Percentage of dehairing after treatment.

Treatment	pH	Incubation time (hour)	Original weight of cow skin (g)	Weight of hair (g)	Percentage of dehairing based on weight (%)
dH ₂ O (control)	7	12	5.4201	0.0026	0.05
Enz + Lime + Sodium Sulfite	7	12	7.9100	0.0455	0.58
Enz + Lime + Sodium Sulfite	7	18	5.9663	0.0592	0.99
Enz + Lime + Sodium sulfite	9	12	8.9724	0.0145	0.16
Enz + Lime + Sodium Sulfite	11	12	6.7822	0.0287	0.43
Sodium Sulfite	9.57	12	6.6840	0.0242	0.36
Lime	12.12	12	6.7310	0.0080	0.12
Lime + Sodium Sulfite	12.51	12	3.8750	-	-
Enz + Lime + Sodium Sulfite + CaCl_2	7	12	6.4939	0.0020	0.03
Enz + Lime + Sodium Sulfite + ZnCl_2	7	12	7.1563	0.0195	0.27

Enz = Enzyme

Similarly, with respect to hair condition, the inclusion of calcium metal resulted in incomplete hair removal and no epidermis adhering to the hair root, which corresponds to the low dehairing activity achieved (Figure 4(B)). This finding suggests that the hair root has been damaged, leaving residue hair on the skin. The breakage may be due to inhibited enzymatic activity,

resulting in no proteoglycan degradation for fibre opening (Sivasubramanian, Manohar & Puvanakrishnan 2008; Sivasubramanian et al. 2008). In contrast, large epidermis residues were observed in the zinc treatment, which indicate complete dehairing (Figure 4(C)). Thus, the lower dehairing activity achieved may be due to the suppression mentioned above, thicker leather, or the use of lesser force when scraping off hair (Zekeya et al. 2019).

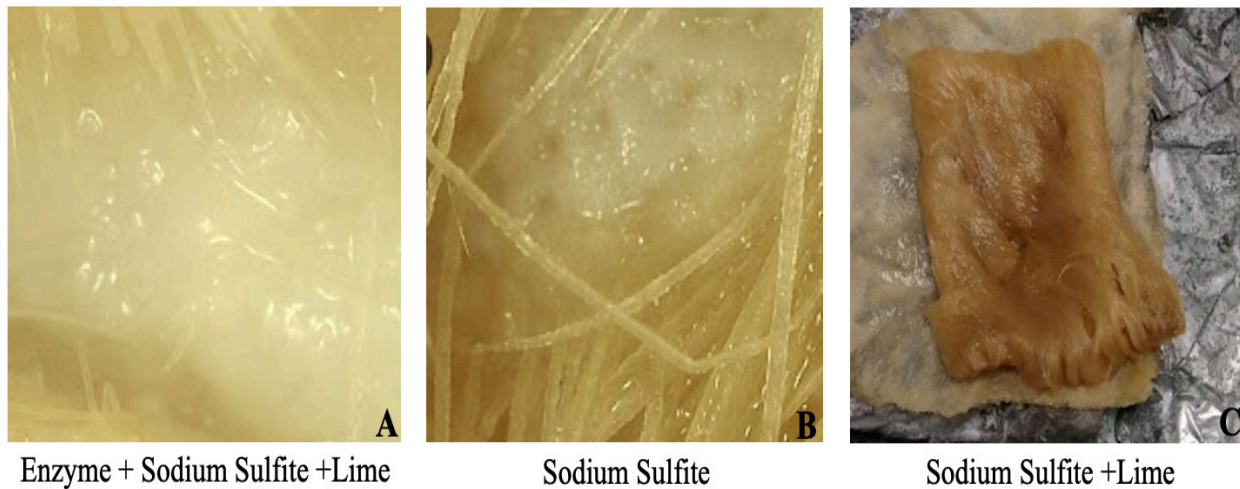


FIGURE 3. Leather conditions after incubation. A) Leather condition after enzyme-chemical treatment. The leather shows smaller pores and a more delicate skin condition. B) Leather condition after sodium sulfite treatment. The leather shows larger pores and a rougher skin condition. C) Leather condition following sodium sulfite and lime treatment. The leather has lost its rigid structure and is easily broken with a little force

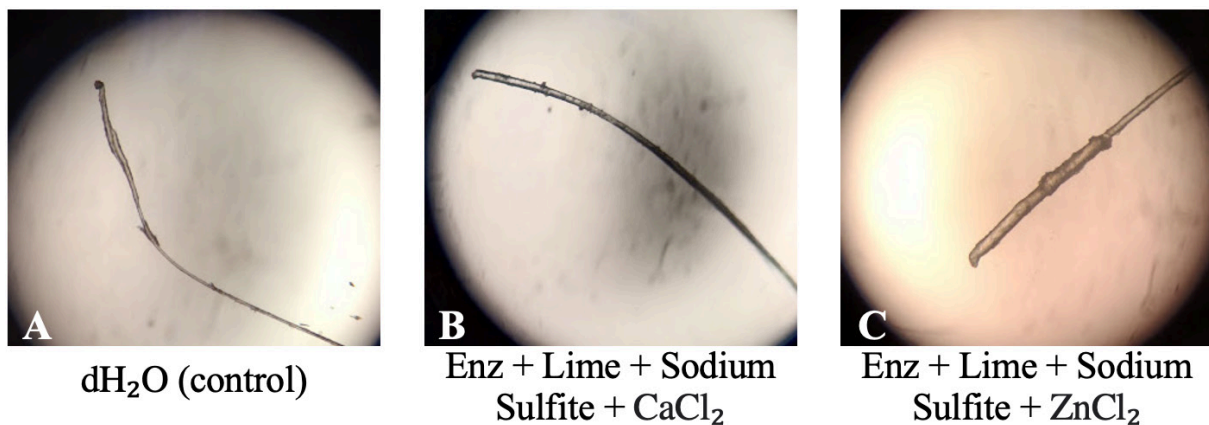


FIGURE 4. Cow hair condition under light microscope. A) Hair appearance after dH₂O incubation. The hair root has a little epidermis attached. B) Hair appearance after incubation with Enzyme + Lime + Sodium Sulfite + CaCl₂. The hair root end was broken. C) Hair appearance after incubation with Enzyme + Lime + Sodium Sulfite + ZnCl₂. Large epidermis content attached to the hair root

CONCLUSIONS

In summary, the most important calcium-binding sites for stability that have been discovered are Tyr171 and Leu75, according to HotSpot Wizard and YASARA, respectively. This finding was a key for future stability improvement in order to overcome subtilisin's susceptibility to degradation. In contrast, Asp41 mutation with HotSpot demonstrated a necessary amendment for future 3D structure refinement of Rand protease. In addition, for dehairing applications, Rand protease-chemical mixtures (with lime and sodium sulfite) had proven their potential to dehair cow skin better than other formulations (including conventional dehairing), which showed best dehairing at pH 7 for 18 h and in the absence of metal ions. They also produce better leather quality. The addition of zinc metal appears to boost epidermis removal, providing cleaner leather, which is demanded by industry. Hence, it was obvious that Rand protease was capable of replacing lime sulfite usage. Future research may use the suggestions of mutations derived from computational analyses to enhance both the activity and stability of Rand protease, thereby improving its potential for practical applications.

ACKNOWLEDGEMENTS

The authors would like to acknowledge the grant GP-IPM/2019/9676800 supported by Universiti Putra Malaysia for funding the project.

REFERENCES

- Abusham, R.A., Rahman, R.N.Z.R.A., Salleh, A.B. & Basri, M. 2009. Optimization of physical factors affecting the production of thermo-stable organic solvent-tolerant protease from a newly isolated halo tolerant *Bacillus subtilis* strain Rand. *Microbial Cell Factories* 8(1): 20.
- Abusham, R.A.K., Masomian, M., Salleh, A.B., Thean, A.C.L. & Rahman, R.N.Z.R.A. 2019. An *in silico* approach to understanding the structure-function: A molecular dynamics simulation study of Rand serine protease properties from *Bacillus subtilis* in aqueous solvents. *Advances in Biotechnology & Microbiology* 12(2): 2474-4637.
- Ahmad, M., Tahir, A. & Anjum, R. 2020. Heat stability of proteins and its exploitation for purification of heat-stable proteins. *Preprints* 2020080225. <https://doi.org/10.20944/preprints202008.0225.v1>
- Azrin, N.A.M., Ali, M.S.M., Rahman, R.N.Z.R.A., Oslan, S.N. & Noor, N.D.M. 2022. Versatility of subtilisin: A review on structure, characteristics, and applications. *Biotechnology and Applied Biochemistry* 69(6): 2599-2616.
- Bendl, J., Stourac, J., Sebestova, E., Vavra, O., Musil, M., Brezovsky, J. & Damborsky, J. 2016. HotSpot Wizard 2.0: Automated design of site-specific mutations and smart libraries in protein engineering. *Nucleic Acids Research* 44(W1): W479-W487.
- Bradford, M.M. 1976. A rapid and sensitive method for the quantitation of microgram quantities of protein utilizing the principle of protein-dye binding. *Analytical Biochemistry* 72(1): 248-254.
- Califano, V. & Costantini, A. 2021. Enzyme immobilization and biocatalysis. *Catalysts* 11(7): 823.
- Chapman, T. 2018. *Sunset 2020 NOSB final review crops substances §205.601, §205.602*. National Organic Standard Board.
- Chen, V.B., Williams, C.J., Headd, J.J., Moriarty, N.W., Prisant, M.G., Videau, L.L., Deis, L.N., Verma, V., Keedy, D.A., Hintze, B.J., Jain, S., Lewis, S.M., Arendall, W.B., Snoeyink, J., Adams, P.D., Lovell, S.C., Richardson, J.S. & Richardson, D.C. 2010. MolProbity: All-atom structure validation for macromolecular crystallography. *Acta Crystallographica D* 66: 12-21.
- Eser, A. & Aydemir, T. 2022. Subtilisin Carlsberg immobilization and its application for eco-friendly leather processing. *Journal of Cleaner Production* 377: 134296.
- Gasteiger, E., Hoogland, C., Gattiker, A., Duvaud, S., Wilkins, M.R., Appel, R.D. & Bairoch, A. 2005. Protein identification and analysis tools on the ExPASy server. In *The Proteomics Protocols Handbook*, edited by Walker, J.M., New Jersey: Humana Press. pp. 571-607.
- Gianfreda, L. & Scarfi, M.R. 1991. Enzyme stabilization: State of the art. *Molecular and Cellular Biochemistry* 100: 97-128.
- Grantham, R. 1974. Amino acid difference formula to help explain protein evolution. *Science* 185(4154): 862-864.
- Hakim, A., Bhuiyan, F.R., Iqbal, A., Emon, T.H., Ahmed, J. & Azad, A.K. 2018. Production and partial characterization of dehairing alkaline protease from *Bacillus subtilis* AKAL7 and *Exiguobacterium indicum* AKAL11 by using organic municipal solid wastes. *Heliyon* 4(6): e00646.
- Jung, Y.E., Lee, K.W., Cho, J.H., Bae, D.W., Jeong, B.G., Jung, Y.J., Park, S.B., An, Y.J., Kim, K., Lee, G.S., Kang, L.W., Moon, J.H., Lee, J.H., Kim, E.K., Yim, H.S. & Cha, S.S. 2023. Heating-mediated purification of active FGF21 and structure-based design of its variant with enhanced potency. *Scientific Reports* 13: 1005.
- Mehrnoosh, A., Mustafa, S. & Yazid, A.M.M. 2011. Heat-treatment aqueous two phase system for purification of serine protease from kesinai (*Streblus asper*) leaves. *Molecules* 16(12): 10202-10213.
- Mohanty, M. & Mohanty, P.S. 2023. Molecular docking in organic, inorganic, and hybrid systems: A tutorial review. *Monatshefte für Chemie* 154: 683-707.

- Mukhtar, H. & Haq, I. 2008. Production of alkaline protease by *Bacillus subtilis* and its application as a depilating agent in leather processing. *Pakistan Journal of Botany* 40(4): 1673-1679.
- Pal, S. & Mitra, R.K. 2022. Investigation on the effect of nonpolar amino acids as macromolecular crowders on the stability of globular proteins. *Chemical Thermodynamics and Thermal Analysis* 6: 100044.
- Schrödinger, L. & DeLano, W. 2020. PyMOL. <http://www.pymol.org/pymol>. Accessed January 2, 2023.
- Shaikh, I.K., Dixit, P.P. & Shaikh, T.M. 2018. Purification and characterization of alkaline soda-bleach stable protease from *Bacillus* sp. APP-07 isolated from Laundromat soil. *Journal of Genetic Engineering and Biotechnology* 16(2): 273-279.
- Sirvaityte, J., Vaitaisi, U. & Jaimaines, G. 2015. *Immunitization Action of Sodium Silicate on Hair: Part 2 Hair-Save Process Based on Lime Substitution by Sodium Silicate* (PCT. Patent No. WO 2021101381A1). International Application Published Under the Patent Cooperation Treaty (PCT). <https://patents.google.com/patent/WO2021101381A1/en>
- Sivasubramanian, S., Manohar, B.M. & Puvanakrishnan, R. 2008. Mechanism of enzymatic dehairing of skins using a bacterial alkaline protease. *Chemosphere* 70(6): 1025-1034.
- Sivasubramanian, S., Manohar, B.M., Rajaram, A. & Puvanakrishnan, R. 2008. Ecofriendly lime and sulfide free enzymatic dehairing of skins and hides using a bacterial alkaline protease. *Chemosphere* 70(6): 1015-1024.
- Suharti, S., Riesmi, M.T., Hidayati, A., Zuhriyah, U.F., Wonorahardjo, S. & Susanti, E. 2018. Enzymatic dehairing of goat skin using keratinase from *Bacillus* sp. MD24, a newly isolated soil bacterium. *Pertanika Journal of Tropical Agricultural Science* 41: 1449-1461.
- Sumbalova, L., Stourac, J., Martinek, T., Bednar, D. & Damborsky, J. 2018. HotSpot Wizard 3.0: web server for automated design of mutations and smart libraries based on sequence input information. *Nucleic Acids Research* 46(W1): W356-W362.
- Suraj, S. & Onkar, S. 2022. *Enzymes Market Statistics, Growth Drivers: Forecast – 2031*. Allied Market Research. <https://www.alliedmarketresearch.com/enzymes-market>. Accessed September 7, 2022.
- Thanikaivelan, P., Rao, J. & Nair, B. 2000. Development of a leather processing method in narrow pH profile: Part 1. Standardisation of dehairing process. *Journal of the Society of Leather Technologists and Chemists* 84: 276-284.
- Ullah, N., Rehman, M.U., Sarwar, A., Nadeem, M., Nelofer, R., Shakir, H.A., Irfan, M., Idrees, M., Naz, S., Nabi, G., Shah, S., Aziz, T., Alharbi, M., Alshammari, A. & Alqahtani, F. 2022. Purification, characterization, and application of alkaline protease enzyme from a locally isolated *Bacillus cereus* strain. *Fermentation* 8(11): 628.
- Vlavianos, C. 2020. *Global SO2 Emissions Drop in 2019 – Greenpeace Global Ranking*. Greenpeace Africa. <https://www.greenpeace.org/africa/en/press/12340/global-so2-emissions-drop-in-2019-greenpeace-global-ranking/>. Accessed July 20, 2022.
- Volza Grow Global. 2023. *Protease Enzyme Imports in Germany*. <https://www.volza.com/p/protease-enzyme/import/import-in-germany/>. Accessed November 9, 2023.
- Ward, O.P. 2011. 3.49- *Proteases in Comprehensive Biotechnology*. 2nd ed. Massachusetts: Academic Press. pp. 571-582. <https://doi.org/https://doi.org/10.1016/B978-0-08-088504-9.00222-1>
- Zekeya, N., China, C., Mbwana, S. & Mtambo, M. 2019. Dehairing of animal hides and skins by alkaline proteases of *Aspergillus oryzae* for efficient processing to leather products in Tanzania. *African Journal of Biotechnology* 18(20): 426-434.

*Corresponding author; email: dina@upm.edu.my

SUPPLEMENTARY FIGURE 21. Influences of various factors on the percentage of dehairing. A) Comparison of the effects of various treatments. B) Comparison of the effects of incubation periods. C) Comparison of the effects of different metal ions. D) Comparison of the effects of different pH levels

Influences of various treatments, incubation time, pH, and types of metal ions on the percentage of dehairing (%)

